Published in final edited form as:
J Am Coll Cardiol. 2014 December 30; 64(25): 2765–2776. doi:10.1016/j.jacc.2014.09.071.

Disturbance in Z-disk mechanosensitive proteins induced by a persistent mutant myopalladin causes familial restrictive cardiomyopathy

Anne-Cecile Huby, PhD[*], **Uzmee Mendsaikhan, MD**[*], **Ken Takagi, MD**[†], **Ruben Martherus, PhD**[*], **Janaka Wansapura, PhD**[‡], **Nan Gong, MD**[*], **Hanna Osinska, PhD**[*], **Jeanne James, MD, PhD**[*], **Kristen Kramer, BS**[*], **Kazuyoshi Saito, MD**[*], **Jeffrey Robbins, PhD**[*], **Zaza Khuchua, PhD**[*], **Jeffrey A. Towbin, MD**[*], and **Enkhsaikhan Purevjav, MD, PhD**[*]

[*]The Heart Institute, Department of Pediatrics, Cincinnati Children's Hospital Medical Center, Cincinnati, Ohio

[†]Jikei University, Tokyo, Japan

[‡]Department of Radiology, Imaging Research Center, Cincinnati Children's Hospital Medical Center, Cincinnati, Ohio

Abstract

BACKGROUND—Familial restrictive cardiomyopathy (FRCM) has a poor prognosis due to diastolic dysfunction and restrictive physiology (RP). Myocardial stiffness, with or without fibrosis, underlie the RP, but the mechanism(s) of restrictive remodeling is unclear. Myopalladin (MYPN) is a messenger molecule that links structural and gene regulatory molecules via translocation from the Z-disk and I-bands to the nucleus in cardiomyocytes. Expression of N-terminal MYPN peptide results in a severe disruption of sarcomere.

OBJECTIVES—A nonsense MYPN-Q529X mutation previously identified in the FRCM family was studied here in an animal model to explore the molecular and pathogenic mechanisms of FRCM.

METHODS—Functional (echocardiography, cardiac magnetic resonance [CMR] imaging, electrocardiography), morphohistological, gene expression, and molecular studies were performed in knock-in heterozygote ($Mypn^{WT/Q526X}$) and homozygote mice harboring the human MYPN-Q529X mutation.

RESULTS—At 12 weeks of age, echocardiographic and CMR imaging signs of diastolic dysfunction with preserved systolic function were identified in $Mypn^{WT/Q526X}$ mice. Histology

Corresponding Author: Enkhsaikhan Purevjav, MD, PHD MLC7020, 3333 Burnet Avenue Cincinnati, OH 45229 Enkhsaikhan.Purevjav@cchmc.org.

Conflict of interest: None

revealed interstitial and perivascular fibrosis without overt hypertrophic remodeling. Truncated Mypn^{Q526X} protein was found to translocate to the nucleus. Levels of total and nuclear cardiac ankyrin repeat protein (Carp/*Ankrd1*) and phosphorylation of Mek1/2, Erk1/2, Smad2, and Akt were reduced. Up-regulation was evident for muscle LIM protein (Mlp), desmin, and heart failure (*Nppa*, *Nppb*, and *Myh6*) and fibrosis (*Tgfβ1*, *αSma*, *Opn*, and *Postn*) markers.

CONCLUSIONS—Heterozygote Mypn$^{WT/Q526X}$ knock-in mice develop RCM due to persistence of mutant Mypn-Q526X protein in the nucleus. Down-regulation of Carp and up-regulation of Mlp and desmin appear to augment fibrotic restrictive remodeling, and reduced Erk1/2 blunts a hypertrophic response in Mypn$^{WT/Q526X}$ hearts.

Keywords

CARP/*ANKRD1*; ERK1/2; fibrosis; remodeling

Introduction

Restrictive cardiomyopathy (RCM) accounts for ~5% of diagnosed cardiomyopathies and is characterized by diastolic dysfunction and restrictive physiology (RP), while systolic function typically remains normal or near normal (1). The volume and wall thickness of the ventricles is usually normal or small, while atrial or bi-atrial enlargement occurs due to impaired ventricular filling during diastole (2). Particularly in children, RCM maintains the poorest prognosis among all types of heart muscle diseases with 2- and 5-year mortality of 50% and 70%, respectively, and the highest rate of sudden cardiac death (SCD) (3). Survivors ultimately develop heart failure (HF) due to RP, as well as pulmonary hypertension; however, the mechanistic basis of restrictive physiology with diastolic dysfunction, myocardial fibrosis, and cardiac stiffness is unclear.

A history of familial RCM (FRCM) is reported in approximately 30% of RCM cases, with autosomal dominant inheritance most commonly noted (4). Several genes, typically encoding proteins of the sarcomere, Z-disk, cytoskeleton, or intermediate filament network, have been associated with autosomal dominant FRCM (4). The myopalladin (*MYPN)* gene, which is located at chromosome 10q21.3, encodes a 145-kDa protein that participates in linking regulatory molecules involved in sarcomeric I-band and Z-disk assembly and muscle gene expression (5). The N-terminal MYPN interacts with cardiac ankyrin repeat protein (CARP/*ANKRD1),* a transcriptional coinhibitor of genes involved in the development of HF and hypertrophy (6). MYPN has dual localization, sarcoplasm, and nucleus similar to that seen with CARP (5). At the Z-disk, MYPN interacts with α-actinin (ACTN2) and with SH3-domain of nebulette (NEBL) (7). Mutations in the *MYPN* gene cause diverse phenotypes in humans, including dilated cardiomyopathy, hypertrophic cardiomyopathy, and restrictive cardiomyopathy (8,9). We have previously reported a nonsense autosomal dominant mutation (*MYPN*-Q529X) that resulted in FRCM in siblings via disturbed myofibrillogenesis and sarcomeric Z-disk disruption (9).

In this study, knock-in mice carrying a heterozygous and homozygous Mypn-Q526X mutation in exon 10 of murine *Mypn* gene, homologous to the human *MYPN*-Q529X

mutation, were analyzed to determine the pathophysiology and molecular mechanism(s) of FRCM.

METHODS

GENERATION OF KNOCK-IN MICE

The study conformed to the protocols approved by the Institutional Animal Care and Use Committee at Cincinnati Children's Hospital Medical Center. To generate a murine Mypn-Q526X mutation, we targeted exon 10 in the *Mypn* gene (**Supplemental Figure 1A**), using a homologous recombination method as described previously (10) and detailed in **Supplemental Materials**.

EVALUATION OF HEART FUNCTION IN MICE

Serial echocardiography and electrocardiography (ECG) was performed in mice at 6 and 12 weeks of age (12 animals/group). Cardiac magnetic resonance (CMR) imaging was performed in 12-week-old animals when mice showed markedly increased E/A (early [E] and late [A] diastolic velocities) ratio, signs of “restrictive filling,” or diastolic dysfunction by echocardiography. See **Supplemental Materials** for experimental details.

HISTOPATHOLOGY, IMMUNOHISTOCHEMISTRY, QUANTITATIVE REAL-TIME PCR, AND ELECTRON MICROSCOPY

Histopathology including H&E, Masson's trichrome, immunohistochemical, transcriptional, and Terminal deoxynucleotidyl transferase dUTP nick end labeling (TUNEL) analysis was performed to assess structural, fibrotic, hypertrophic, and/or apoptotic remodeling in the heart. Transmission electron microscopy (TEM) was performed on glutaraldehyde-perfused hearts as previously described (11). After isolation of total ribonucleic acid (RNA) from ventricular tissues, quantitative real-time polymerase chain reaction (PCR) was performed as described in **Supplemental Materials**. Six 12-week-old animals/group were used. See experimental details in **Supplemental Materials**.

PROTEIN EXPRESSION, PULL-DOWN AND WESTERN BLOTTING

Human embryonic kidney (HEK293) cells were transfected with different chimeras of MYPN-GFP and CARP-V5 complementary deoxyribonucleic acids (cDNAs) to evaluate MYPN and CARP interactions using immunoprecipitation (IP) and co-immunoprecipitation (Co-IP). Cellular fractionation was performed using the NE-PER kit (Pierce, Rockford, Illinois). Western blotting was used for protein evaluation and levels of proteins were quantified in relative density units using ImageJ software as described in **Supplemental Materials**.

STATISTICAL ANALYSIS

Statistical analysis reported as mean ± structural equation modeling was performed with Student *t* test or 1-way analysis of variance using GraphPad5 software (GraphPad Software, Inc., La Jolla, California). A probability value of $p \leq 0.05$ was considered significant.

RESULTS

MANIFESTATION OF DIASTOLIC DYSFUNCTION

Given that persistence of 65-kDa-Mypn^{Q526X} peptide in vivo may potentially cause a "poison peptide" effect, levels of the Mypn protein were confirmed by Western blotting; the Mypn$^{WT/Q526X}$ line #3 with the highest 65-kDa-Mypn^{Q526X} protein expression was selected for further breeding (**Supplemental Figure 1B**). Heterozygous and homozygous recombination of the Mypn-Q526X mutation was confirmed by sequencing of *Mypn* exon 10 in genomic DNA obtained from mouse tails (**Supplemental Figure 1C**). We verified *Mypn* messenger RNA (mRNA) transcription levels in the heart, skeletal muscle, liver, and kidneys by reverse transcription PCR. As expected, homozygotes had impaired *Mypn* mRNA transcription in heart and skeletal muscle compared to wild-type (WT) and heterozygote littermates (**Supplemental Figure 1D-E**). Thus, homozygous Mypn^{Q526X} mice were also generated to utilize as a model of *Mypn* gene ablation.

Both Mypn$^{WT/Q526X}$ and Mypn^{Q526X} mice were born and grew normally, with no skeletal myopathy observed up to 12 weeks of age. At 6 weeks, increased E/A ratios, features of RP in humans (12), were detected in Mypn$^{WT/Q526X}$ mice compared to WT and homozygotes. The same cohort of mice underwent a serial echocardiography at 12 weeks of age and an increase in the E/A ratio became significantly profound (**Figure 1A**). While systolic function and chamber dimensions were preserved, Mypn$^{WT/Q526X}$ mice showed signs of impaired diastolic filling of the left ventricle (LV), including decreased end-diastolic volume (LVEDV) and internal dimensions compared to WT and homozygotes (**Supplemental Table 1**).

Further, CMR imaging was utilized in the same cohort of 12-week-old mice to precisely evaluate cardiac anatomy and diastolic function. No significant differences between groups were found in circumferential strain, strain rate, torsion, or torsion rate (data not shown). The left atrial cross-sectional area of Mypn$^{WT/Q526X}$ mice (3.8 ± 0.5 mm^2) was larger compared to WT mice (3.5 ± 0.6 mm^2) and homozygotes (3.0 ± 0.3 mm^2, $p = 0.02$) as measured in the 4-chamber view (**Figure 1B and Supplemental Table 2**). The LVEDV was significantly lower in the Mypn$^{WT/Q526X}$ mutants compared to WT mice ($p = 0.03$). The sphericity index, the ratio of the short- to long-axis dimensions of the LV, was also lower in the Mypn$^{WT/Q526X}$ mice (0.51 ± 0.03) compared to WT animals (0.56 ± 0.03; $p = 0.02$), consistent with LV remodeling in heterozygotes only.

Arrhythmias and conduction abnormalities are reportedly present in 15% to 30% of RCM patients, especially in pediatric patients (13). ECGs revealed that heart rate, P, PR, and QRS durations were similar among mutant and WT mice, while T wave duration was decreased in Mypn$^{WT/Q526X}$ versus WT or homozygotes (**Supplemental Table 3**). Arrhythmias including premature atrial contractions, premature ventricular contractions, and type II second-degree atrioventricular block (**Figure 1C**) were observed in heterozygotes only.

FIBROSIS IN HETEROZYGOUS MYPN$^{WT/Q526X}$ HEARTS

Morphologic evaluation of cardiac muscle revealed no hypertrophy in any animal (**Figure 2A**). Histologically, diffuse interstitial and perivascular fibrosis was found in Mypn$^{WT/Q526X}$ ventricular myocardium only. Dystrophin staining revealed intact sarcolemmal integrity and normal cardiomyocyte size among the different groups, confirming absence of cardiomyocyte hypertrophy (**Supplemental Figure 2A**). No positive TUNEL staining was seen in any group, excluding the involvement of apoptosis. Ultrastructurally, t-tubules enlargement and mild intercalated disk disruption was seen in heterozygous and homozygous animals (**Figure 2B**).

Taken together, these results show that heterozygote Mypn$^{WT/Q526X}$ mutants demonstrated fibrotic remodeling without an overt hypertrophic response, accurately recapitulating the human RCM phenotype. Homozygous Mypn^{Q526X} mice had no or a minimal phenotype as result of MYPN^{Q526X} ablation. Therefore, further comparative molecular studies were carried out in Mypn$^{WT/Q526X}$ and WT littermates.

PUTATIVE Z-DISK STRESS-SENSOR DYSREGULATION IN MYPN$^{WT/Q526X}$ HEARTS

Immunohistochemical analysis revealed no differences in MYPN at the Z-disks. Notably, coincident de-localization of Carp and desmin to the periphery was found in Mypn$^{WT/Q526X}$ cardiomyocytes only (**Figure 3, arrows**). On a protein level, while no Mypn^{WT} was seen, the 65kDa-Mypn^{Q526X} was detected in the hearts of heterozygous mice as expected (**Figure 4A**). A significant increase in the expression of the Mypn's homolog, palladin (90kDa), was evident in Mypn$^{WT/Q526X}$ hearts and confirmed by monoclonal antibody and immunohistochemical staining (**Supplemental Figure 2B**). Nebulette and α-actinin2 were mildly up-regulated, whereas Carp was considerably down-regulated in Mypn$^{WT/Q526X}$ ($p = 0.03$). Levels of calpain3 were similar in mutants and WT, excluding the likelihood of Carp degradation due to increased protease activation. Desmin and muscle LIM protein (Mlp/Csrp3), the putative Z-disk stress-sensors, were significantly up-regulated in heterozygotes versus WT ($p < 0.05$). Mild down-regulation of α-tubulin, caveolin-3, and vinculin occurred in Mypn$^{WT/Q526X}$ compared to WT, suggesting an early recruitment of t-tubules and adherens junctions, respectively (**Supplemental Figure 2B**). Intercalated disk proteins such as desmoplakin2, connexin43, or N-cadherin were not affected. Levels of cardiac troponin I (cTnI) and phospho-cTnI were normal, consistent with intact sarcomeres.

ANALYSIS OF DOWNSTREAM SIGNALING PATHWAYS

As cardiac stretch is regulated mainly at the Z-disks by extracellular-signal-regulated kinase (ERK)2-dependent phosphorylation of titin at the Zis1/Z-repeats (14), we sought to determine whether the ERK cascade is altered. Reduced phosphorylated-MAPK/ERK1/2 (p-Mek1/2) and p-Erk1/2 was seen in Mypn$^{WT/Q526X}$ hearts compared to WT (**Figure 4B**), while other potential mitogen-activated protein kinase (MAPK)-associated targets, including p-53, c-Jun N-terminal kinase, p-38, focal adhesion kinase, nuclear factor kappa-light-chain-enhancer of activated B cells, signal transducer and activator of transcription 3, ERBB4, and transforming growth factor-β1, were not affected (**Supplemental Figure 2C**). Phosphorylation of Smad2 and Akt was reduced in Mypn$^{WT/Q526X}$ animals, however.

Further, CARP-dependent genes including *Nppa*, *Nppb*, and *Myh6* mRNA (**Supplemental Table 4**) were elevated in Mypn$^{WT/Q526X}$ hearts, supporting the idea of diminished inhibitory effects of CARP due to reduced levels of CARP protein (**Figure 4C**). Significant increases in fibrotic (*αSma*, *Tgf-β1*, *Postn* and *Opn*), inflammatory (*Vcam*, *Icam* and*Il-1β*), and antiapoptotic (*Bcl-2*) genes were identified in Mypn$^{WT/Q526X}$ hearts.

PERSISTENCE OF NUCLEAR 65KDA-MYPN PEPTIDE ASSOCIATED WITH RCM PHENOTYPE

To determine whether the location and expression levels of proteins are associated with the RCM phenotype in vivo, mouse hearts from all groups (WT and heterozygote and homozygote mutants) were fractionated and levels of total, nuclear, and cytoplasmic Mypn, palladin, and Carp were quantitated. Comparable expression of nuclear palladin was documented in all groups (**Figure 5A**), excluding the likelihood of pathologic effects of increased palladin in the nucleus. Interestingly, the 65kDa-Mypn^{Q526X} peptide was detected in the nuclear fraction of heterozygote hearts and very little amount in homozygotes, suggesting a potential cause of the RCM phenotype. A concordant decrease in total Carp levels was detected in Mypn$^{WT/Q526X}$ hearts.

To further clarify MYPN-CARP interactions, different combinations of human MYPN^{WT} and MYPN^{Q529X} cDNAs fused with green fluorescent protein (GFP) or mixtures of both MYPN^{WT} and MYPN^{Q529X} (MYPN$^{WT/Q529X}$) were co-transfected with human CARP-V5 construct in HEK293 cells and pulled down. As shown in **Figure 5B**, GFP antibody pulled down the 65kDa-MYPN^{Q529X} as did the 145kDa-MYPN^{WT} in all transfected cells, except control and CARP-transfected ones. In contrast, levels of V5-pulled 40kDa-CARP were reduced in MYPN^{Q529X} cells compared to MYPN^{WT}. Further, the 40kDa-CARP-V5 was undetectable in MYPN$^{WT/Q529X}$ mixed lysates presumably due to greater levels in reduction of CARP expression compared to mutant MYPN^{Q529X} cells. These effects support the in vivo data of reduced murine Carp levels in heterozygous hearts and the idea that nuclear 65kDa-Mypn^{Q526X} may suppress Carp expression.

Subsequently, levels of *Carp*, *Mlp*, and *Des* mRNA were evaluated in the myocardial tissues of heterozygote and homozygote mice to further elucidate whether differential phenotypes are associated with nuclear Mypn^{Q526X}-mediated alteration in transcriptional activities of mechanosensitive molecules. As shown in **Figure 5C**, divergent changes in *CARP* mRNA levels were detected in Mypn$^{WT/Q529X}$ and Mypn^{Q529X} hearts compared to WT controls. *Carp* transcription was reduced in Mypn$^{WT/Q529X}$, while Mypn^{Q529X} mice presented *Carp* up-regulation, and this variation between mutants was statistically significant. In contrast, no significant difference in transcription of *Mlp* and *Des* is revealed in any groups.

DISCUSSION

The characteristic features of autosomal dominant familial RCM result in a high-risk disorder with poor clinical outcomes including HF, arrhythmias, and SCD (2). These features include diastolic dysfunction and restrictive ventricular filling, with limited ability to augment cardiac stroke volume due to increased myocardial stiffness and interstitial fibrosis; however, a mechanistic etiology remains unclear (4). MYPN is a sarcomeric

protein localized at the Z-disk, I band, and nucleus. Expression of the N-terminal region of MYPN in cardiomyocytes resulted in severe disruption of the sarcomere (5), while N-terminal mutation MYPN-Y20C reduced CARP-MYPN binding and caused hypertrophic cardiomyopathy in vivo (**Central Illustration**) *via* perturbed MYPN nuclear shuttling and abnormal assembly of terminal Z-disks within intercalated disks (9). Mutations in *MYPN*, therefore, cause diverse cardiomyopathic phenotypes within a critical "final common pathway" (9,15).

The objectives of this study were to uncover the molecular pathogenetic mechanism(s) and discover the associated key signaling molecules in MYPN-Q529X mutation-induced restrictive remodeling using a knock-in mouse model. We demonstrated that homozygous $Mypn^{Q526X}$ mice display no phenotype due to ablation of mutant protein. Heterozygous $Mypn^{WT/Q526X}$ mutants, corresponding to a human heterozygous MYPN-Q529X mutation, recapitulated the clinical and pathologic features of human FRCM, including diastolic dysfunction with preserved systolic function by 12 weeks of age. Interstitial and perivascular fibrosis was seen before overt cardiac contractile dysfunction, while myocyte hypertrophy, apoptosis, and necrosis were absent.

From these data, we hypothesize that the RCM phenotype results from persistence of dysfunctional truncated $Mypn^{Q526X}$ protein and consequent multiple pathological "hits." First, $Mypn^{Q526X}$ translocates to the nucleus, probably perturbing levels of Carp expression (**Central Illustration**). Second, $Mypn^{Q526X}$ causes alterations in Mlp/cysteine-rich protein 3(Csrp3) and desmin and blunts the phosphorylation of Mek1/2-Erk1/2, likely, via negative nuclear feedback. Further, activation of Smad2 and of Akt are reduced, likely to compensate the mutation-induced "final common pathway" of RCM (15).

Balanced levels of CARP are reported to be essential for proper adaptive responses to different stresses in striated muscle (**Central Illustration**), including exercise (16), stretch (17), cytokines (18), hypoxia (19), adrenergic stress (20), and anthracycline (doxorubicin) toxicity (21). Multiple mechanisms, including 26S-proteosome degradation, TGF-β-SMADs, and caspase3 and calpain3 proteases, are reported as CARP regulators (22). Ablation of all forms of muscle ankyrin repeat proteins (MARPs), including CARP, enhances the MyoD and MLP expression in skeletal muscle (23). While ablation of CARP or MARPs has been shown to not affect the cardiac function similar to our $Mypn^{Q526X}$ homozygotes (24), cardiac-restricted CARP over-expression results in an inhibition of hypertrophic and fibrotic remodeling *via* reduced TGF-β and ERK1/2 (18). Our previous $Mypn^{Y20C}$ transgenic mouse model (**Central Illustration**) suggested a crucial role of nuclear WT-Mypn by demonstrating the development of hypertrophic cardiomyopathy in vivo as a result of perturbed nuclear shuttling of Mypn (9). In the present $Mypn^{WT/Q526X}$ model, the mutant $Mypn^{Q526X}$ translocates to the nucleus, reducing the expression of Carp. Transcription of key fibrotic molecule, *Tgf-β1* was up-regulated, but Tgf-β1 protein levels were not changed, and Smad2 was down-regulated, suggesting an alternative TGF-β-SMAD-independent fibrotic pathway. Increased 90kDa-palladin was shown to induce alpha-smooth muscle actin (*a*Sma) through Tgf-β1 and Erk1/2 activation (25), whereas decreased Ankrd2 and Mlp/Csrp3 levels were reported in forced skeletal muscle inactivity in mice (26). Therefore, decreased Carp and elevated Mlp/Csrp3 and Des likely led to fibrosis via

Postn and *Opn* in our model (17). Moreover, up-regulation of *Icam*, *Vcam*, and *Il-1b* in mutants may contribute to perivascular fibrosis (27).

We hypothesize that the net result of decreased Erk1/2, Smads, and Akt signaling may blunt the hypertrophic response in heterozygotes (**Figure 5C**). As Carp has been shown to regulate the Erk2-dependent titin-PEVK spring force at the I-band, we assume that reduction in Mek1/2-Erk1/2 phosphorylation might have a negative feedback origin through the nuclear Mypn^{Q526X}-induced perturbation of mechanosensitive proteins: Carp, Mlp, and Des (28).

In summary, we demonstrate that the 65kDa-Mypn^{Q526X} peptide causes diastolic dysfunction without contractile impairment via net changes in the mechanosensory proteins. To date, no pharmacologic therapies have been shown to clearly improve outcomes in RCM patients, with heart transplantation being the definitive treatment option for many, especially in childhood (29). If our murine findings mirror the pathologic hallmarks of RCM in humans, it could explain why the TGF-β1 suppressor angiotensin-converting enzyme (ACE) inhibitors, β-blockers, and angiotensin receptor blockers (ARBs) are ineffective in RCM patient treatment (3). Further studies on time-dependent expression changes in CARP, MLP, DES, and ERK1/2 in RCM patients may provide useful information for discovering diagnostic and therapeutic targets.

Supplementary Material

Refer to Web version on PubMed Central for supplementary material.

Acknowledgements

We thank Dr. Siegfried Labeit (Klinikum Mannheim, Mannheim, Germany) for providing antibodies against myopalladin and nebulette.

Funding sources: This work was supported in part by a research grants from the American Heart Association, Children's Cardiomyopathy Foundation (EP, JAT), the John Patrick Albright Foundation and NIH-NHLBI (R01 HL53392 and R01 HL087000) (JAT).

ABBREVIATIONS

CARP	cardiac ankyrin repeat protein
CMR	cardiac magnetic resonance
ECG	electrocardiography
HF	heart failure
MLP	muscle LIM protein
MYPN	myopalladin
RCM	restrictive cardiomyopathy
SCD	sudden cardiac death

REFERENCES

1. Maron BJ, Towbin JA, Thiene G, et al. Contemporary definitions and classification of the cardiomyopathies: an American Heart Association Scientific Statement from the Council on Clinical Cardiology, Heart Failure and Transplantation Committee; Quality of Care and Outcomes Research and Functional Genomics and Translational Biology Interdisciplinary Working Groups; and Council on Epidemiology and Prevention. Circulation. 2006; 113:1807–16. [PubMed: 16567565]
2. Maskatia SA, Decker JA, Spinner JA, et al. Restrictive physiology is associated with poor outcomes in children with hypertrophic cardiomyopathy. Pediatr Cardiol. 2012; 33:141–9. [PubMed: 21892651]
3. Webber SA, Lipshultz SE, Sleeper LA, et al. Outcomes of restrictive cardiomyopathy in childhood and the influence of phenotype: a report from the Pediatric Cardiomyopathy Registry. Circulation. 2012; 126:1237–44. [PubMed: 22843787]
4. Sen-Chowdhry S, Syrris P, McKenna WJ. Genetics of restrictive cardiomyopathy. Heart Fail Clin. 2010; 6:179–86. [PubMed: 20347786]
5. Bang ML, Mudry RE, McElhinny AS, et al. Myopalladin, a novel 145-kilodalton sarcomeric protein with multiple roles in Z-disc and I-band protein assemblies. J Cell Biol. 2001; 153:413–27. [PubMed: 11309420]
6. Mikhailov AT, Torrado M. The enigmatic role of the ankyrin repeat domain 1 gene in heart development and disease. Int J Dev Biol. 2008; 52:811–21. [PubMed: 18956313]
7. Ma K, Wang K. Interaction of nebulin SH3 domain with titin PEVK and myopalladin: implications for the signaling and assembly role of titin and nebulin. FEBS Lett. 2002; 532:273–8. [PubMed: 12482578]
8. Duboscq-Bidot L, Xu P, Charron P, et al. Mutations in the Z-band protein myopalladin gene and idiopathic dilated cardiomyopathy. Cardiovasc Res. 2008; 77:118–25. [PubMed: 18006477]
9. Purevjav E, Arimura T, Augustin S, et al. Molecular basis for clinical heterogeneity in inherited cardiomyopathies due to myopalladin mutations. Hum Mol Genet. 2012; 21:2039–53. [PubMed: 22286171]
10. Liu P, Jenkins NA, Copeland NG. A highly efficient recombineering-based method for generating conditional knockout mutations. Genome Res. 2003; 13:476–84. [PubMed: 12618378]
11. Maiellaro-Rafferty K, Wansapura JP, Mendsaikhan U, et al. Altered regional cardiac wall mechanics are associated with differential cardiomyocyte calcium handling due to nebulette mutations in preclinical inherited dilated cardiomyopathy. J Mol Cell Cardiol. 2013; 60C:151–60. [PubMed: 23632046]
12. Jean-Charles PY, Li YJ, Nan CL, Huang XP. Insights into restrictive cardiomyopathy from clinical and animal studies. J Geriatr Cardiol. 2011; 8:168–83. [PubMed: 22783303]
13. Walsh MA, Grenier MA, Jefferies JL, Towbin JA, Lorts A, Czosek RJ. Conduction abnormalities in pediatric patients with restrictive cardiomyopathy. Circ Heart Fail. 2012; 5:267–73. [PubMed: 22260945]
14. Gautel M, Goulding D, Bullard B, Weber K, Furst DO. The central Z-disk region of titin is assembled from a novel repeat in variable copy numbers. J Cell Sci. 1996; 109:2747–54. [PubMed: 8937992]
15. Bowles NE, Bowles KR, Towbin JA. The “final common pathway” hypothesis and inherited cardiovascular disease. The role of cytoskeletal proteins in dilated cardiomyopathy. Herz. 2000; 25:168–75. [PubMed: 10904835]
16. Chen YW, Nader GA, Baar KR, Fedele MJ, Hoffman EP, Esser KA. Response of rat muscle to acute resistance exercise defined by transcriptional and translational profiling. J Physiol. 2002; 545:27–41. [PubMed: 12433947]
17. Mohamed JS, Boriek AM. Loss of desmin triggers mechanosensitivity and up-regulation of Ankrd1 expression through Akt-NF-kappaB signaling pathway in smooth muscle cells. Faseb J. 2012; 26:757–65. [PubMed: 22085644]

18. Song Y, Xu J, Li Y, et al. Cardiac ankyrin repeat protein attenuates cardiac hypertrophy by inhibition of ERK1/2 and TGF-beta signaling pathways. PLoS One. 2012; 7:e50436. [PubMed: 23227174]
19. Lee MJ, Kwak YK, You KR, Lee BH, Kim DG. Involvement of GADD153 and cardiac ankyrin repeat protein in cardiac ischemia-reperfusion injury. Mol Med. 2009; 41:243–52.
20. Zolk O, Marx M, Jackel E, El-Armouche A, Eschenhagen T. Beta-adrenergic stimulation induces cardiac ankyrin repeat protein expression: involvement of protein kinase A and calmodulin-dependent kinase. Cardiovasc Res. 2003; 59:563–72. [PubMed: 14499857]
21. Chen B, Zhong L, Roush SF, et al. Disruption of a GATA4/Ankrd1 signaling axis in cardiomyocytes leads to sarcomere disarray: implications for anthracycline cardiomyopathy. PLoS One. 2012; 7:e35743. [PubMed: 22532871]
22. Kanai H, Tanaka T, Aihara Y, et al. Transforming growth factor-beta/Smads signaling induces transcription of the cell type-restricted ankyrin repeat protein CARP gene through CAGA motif in vascular smooth muscle cells. Circ Res. 2001; 88:30–6. [PubMed: 11139470]
23. Barash IA, Bang ML, Mathew L, Greaser ML, Chen J, Lieber RL. Structural and regulatory roles of muscle ankyrin repeat protein family in skeletal muscle. Am J Physiol Cell Physiol. 2007; 293:C218–27. [PubMed: 17392382]
24. Bang ML, Gu Y, Dalton ND, Peterson KL, Chien KR, Chen J. The Muscle Ankyrin Repeat Proteins CARP, Ankrd2, and DARP Are Not Essential for Normal Cardiac Development and Function at Basal Conditions and in Response to Pressure Overload. PLoS One. 2014; 9:e93638. [PubMed: 24736439]
25. Ronty MJ, Leivonen SK, Hinz B, et al. Isoform-specific regulation of the actin-organizing protein palladin during TGF-beta1-induced myofibroblast differentiation. J Invest Dermatol. 2006; 126:2387–96. [PubMed: 16794588]
26. Roberts MD, Childs TE, Brown JD, Davis JW, Booth FW. Early depression of Ankrd2 and Csrp3 mRNAs in the polyribosomal and whole tissue fractions in skeletal muscle with decreased voluntary running. J Appl Physiol. 2012; 112:1291–9. [PubMed: 22282489]
27. Wilhelmi MH, Leyh RG, Wilhelmi M, Haverich A. Upregulation of endothelial adhesion molecules in hearts with congestive and ischemic cardiomyopathy: immunohistochemical evaluation of inflammatory endothelial cell activation. Eur J Cardiothorac Surg. 2005; 27:122–7. [PubMed: 15621483]
28. Witt SH, Labeit D, Granzier H, Labeit S, Witt CC. Dimerization of the cardiac ankyrin protein CARP: implications for MARP titin-based signaling. J Muscle Res Cell Motil. 2005; 26:401–8. [PubMed: 16450059]
29. Denfield SW, Webber SA. Restrictive cardiomyopathy in childhood. Heart Fail Clin. 2010; 6:445–52. viii. [PubMed: 20869645]

PERSPECTIVES

COMPETENCY IN MEDICAL KNOWLEDGE: Restrictive myocardial remodeling is responsible for the diastolic ventricular dysfunction that characterizes familial restrictive cardiomyopathy (FRCM), which carries a poor prognosis, particularly in affected children. No pharmacological therapies have been found that clearly improve clinical outcomes in patients with this disorder, leaving few alternatives to cardiac transplantation.

TRANSLATIONAL OUTLOOK: This study discovered early molecular markers of restrictive remodeling in a murine model of FRCM that cause diastolic dysfunction without contractile impairment. This points the way toward future studies by which the expression of genes regulating mechanosensory proteins could be modified as potential therapeutic targets.

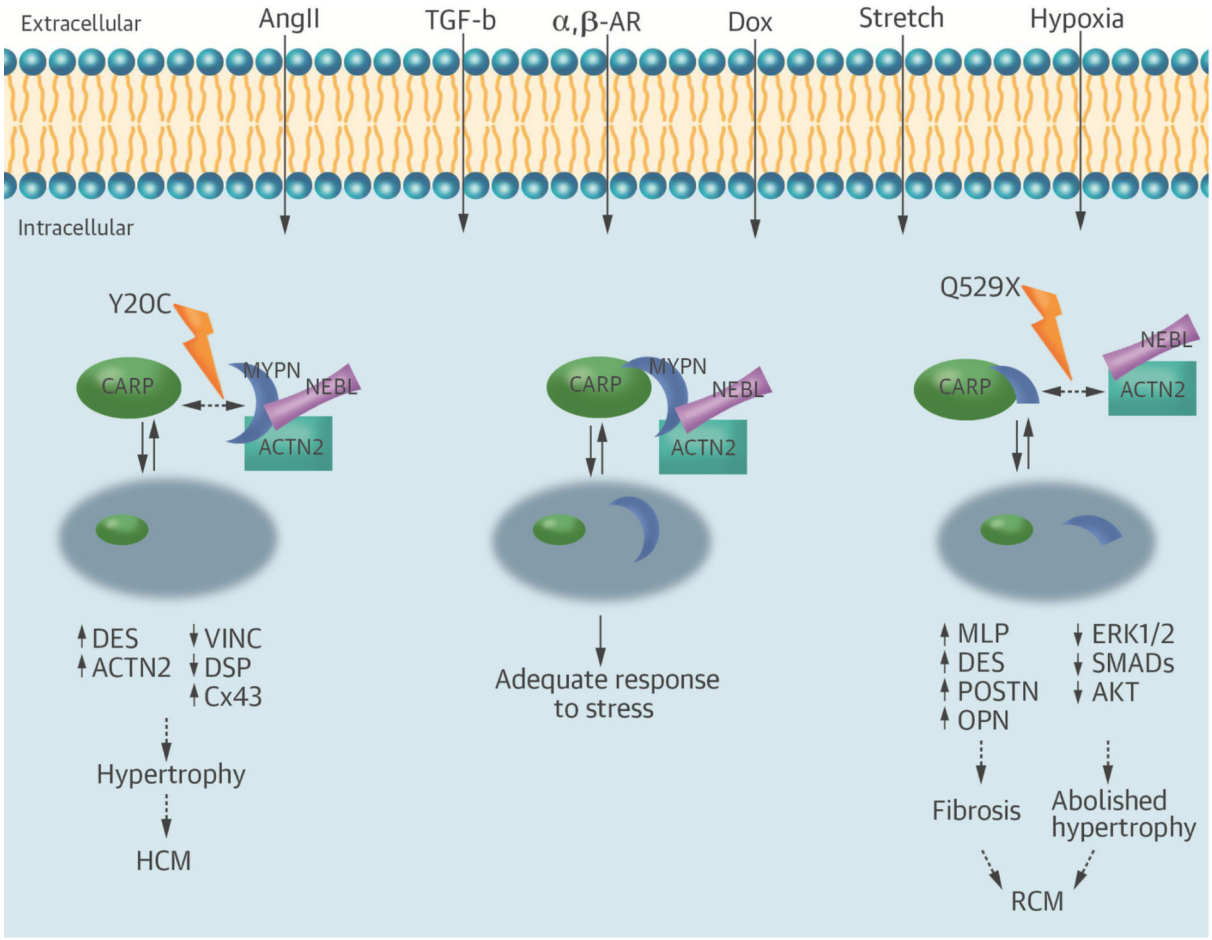

CENTRAL ILLUSTRATION. MYPN-mutation Induced Abnormal Response to Physiological and Pathological Stimuli

Illustrated model of MYPN-mutation induced abnormal response to physiological and pathological stimuli. In this model, the middle panel represents normal, balanced MYPN interactions that regulate adequate response to various stresses. In the MYPN-Q529X-mutation induced RCM, $MYPN^{Q529X}$ peptide (right panel) translocates to the nucleus, decreases CARP expression, and increases MLP and DES on a protein level, leading to fibrosis via up-regulated *POSTN* and *OPN*. The hypertrophic response is abolished *via* reduced ERK1/2, SMADs, and AKT. Limited or loss of adaptive responses to various stimuli results in the development of RCM. Conventional cardiovascular drugs, including ACE inhibitors, ARBs, and β-blockers, thus, have limited effect in patients with RCM. The left panel represents the mechanism of MYPN-Y20C-mutation induced HCM as result of reduced binding of CARP to $MYPN^{Y20C}$ peptide and impaired nuclear translocation of MYPN. Subsequent alterations in DES, ·-actinin, and vinculin, desmoplakin and connexin43 were evident.

ACTN2 = ·-actinin; ACE = angiotensin-converting enzyme; AngII=angiotensin II; ARB = angiotensin II receptor blocker; β-AR = alpha- and beta-adrenergic receptors; CARP = cardiac ankyrin repeat protein; Cx43 = connexin43; DES = desmin; Dox=doxorubicin; DSP = desmoplakin; HCM = hypertrophic cardiomyopathy; MYPN = myopalladin; RCM = restrictive cardiomyopathy; TGF-β = transforming growth factor beta; VIN = vinculin.

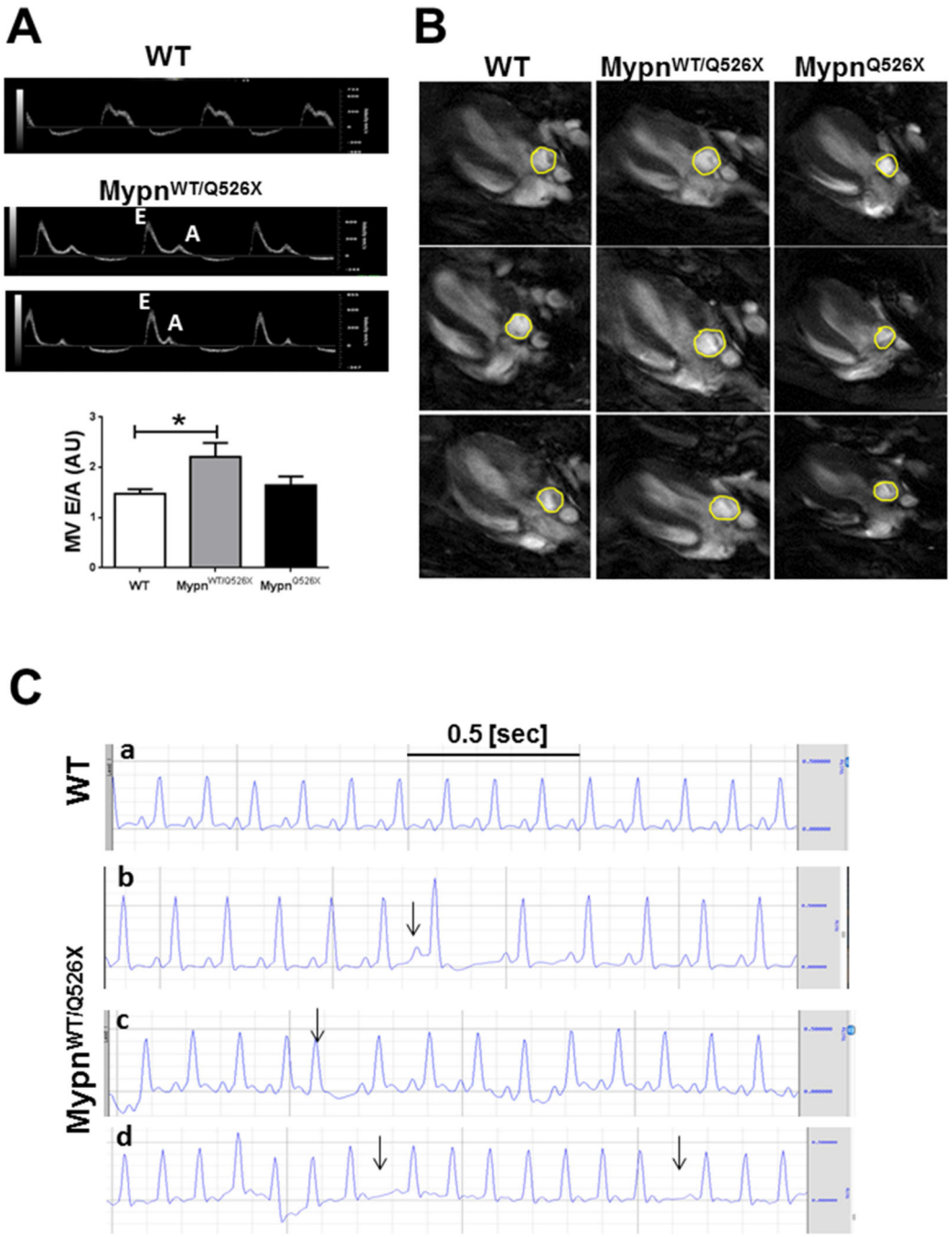

FIGURE 1. Phenotypic Characterization of Mypn Mice

(A) M-mode images of mitral valve movement by 2-dimensional echocardiography indicate an increase of E/A ratios in Mypn$^{WT/Q526X}$ compared to WT or homozygotes, which became significant in 12-week-old heterozygote mutants (grey column) compared to WT and homozygote mice. **(B)** Cardiac magnetic resonance (CMR) images in the 4-chamber view demonstrate enlarged left atria in Mypn$^{WT/Q526X}$ mice (middle columns) compared to WT (left columns) and Mypn^{Q526X} (right columns) mice. **(C)** Electrocardiography in mice. Mypn$^{WT/Q526X}$ mice display arrhythmias (arrows), including (b) premature atrial

contractions, (c) premature ventricular contractions, and 2° atrioventricular block (d; 1:7 Wenkebach).

*$p < 0.05$.

E/A = early [E] and late [A] diastolic velocities; Mypn = myopalladin; WT = wild-type.

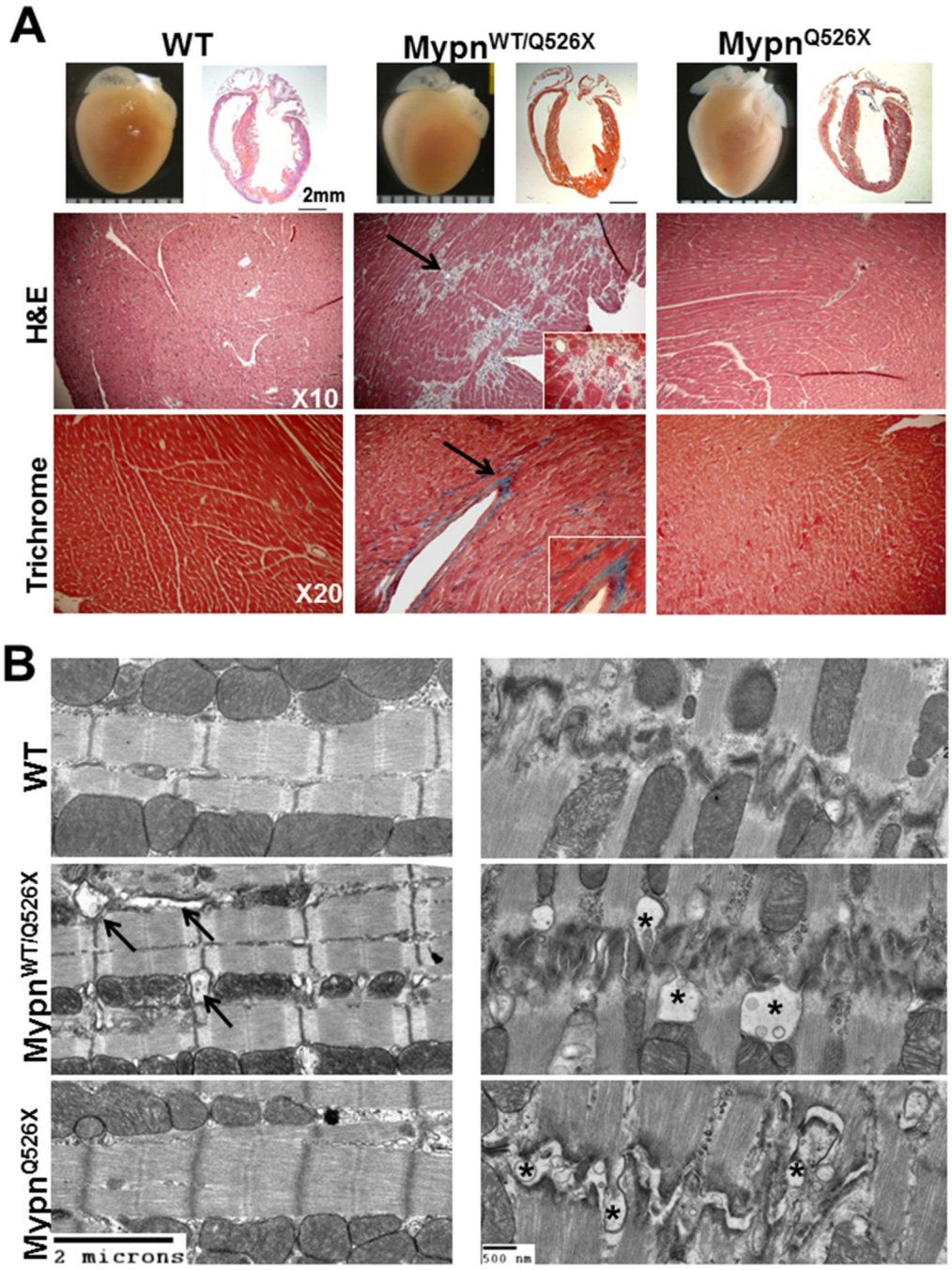

FIGURE 2. Morphohistology of Hearts from 12-week-old Mice

(A) No significant chamber enlargement or cardiac muscle hypertrophy is seen in all groups (upper panels). Sections stained with hematoxylin and eosin (H&E; 10X magnification) demonstrate significant interstitial and perivascular infiltration in the Mypn$^{WT/Q526X}$ myocardium (middle panel) with focal loss of myofibrils (arrow) compared to WT (left panel) and homozygotes (right panel). Masson trichrome staining (X20 magnification) reveals interstitial and perivascular fibrosis in Mypn$^{WT/Q526X}$ myocardium. Right lower panel displays enlarged details. (**B)** Transmission electron microscopy demonstrates no

difference in the sarcomeric and Z-disk organization between groups (left panels, 24,000X magnification). Enlarged t-tubules (arrows) and widened cell-cell junctions with excess convolutions (asterisks) in both mutants are shown. Abbreviations as in **Figure 1**.

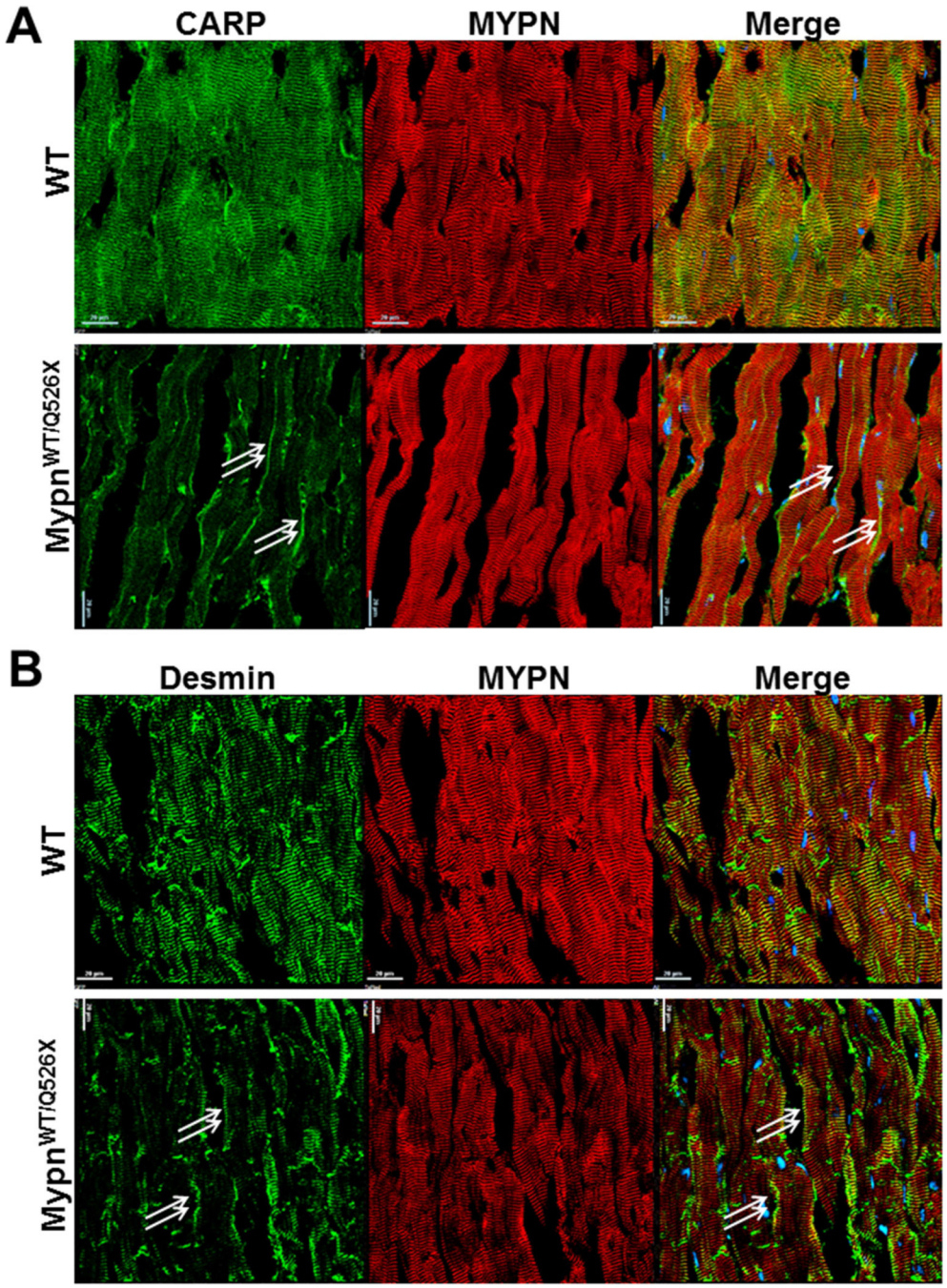

FIGURE 3. Immunohistochemistry of Mouse Hearts

MYPN (red) was co-immunostained with CARP **(A)** and DES **(B)**, both shown in green. Right panels represent the merged images with DAPI (blue). Although no changes in MYPN localization are noted, the striated co-staining pattern in yellow was lost in $Mypn^{WT/Q526X}$ hearts, indicating de-localization of CARP and DES from the cytosol to the periphery of cardiomyocytes (arrows).

CARP = cardiac ankyrin repeat protein; DAPI = diamidino-2-phenylindole; DES = desmin; other abbreviations as in **Figure 1**.

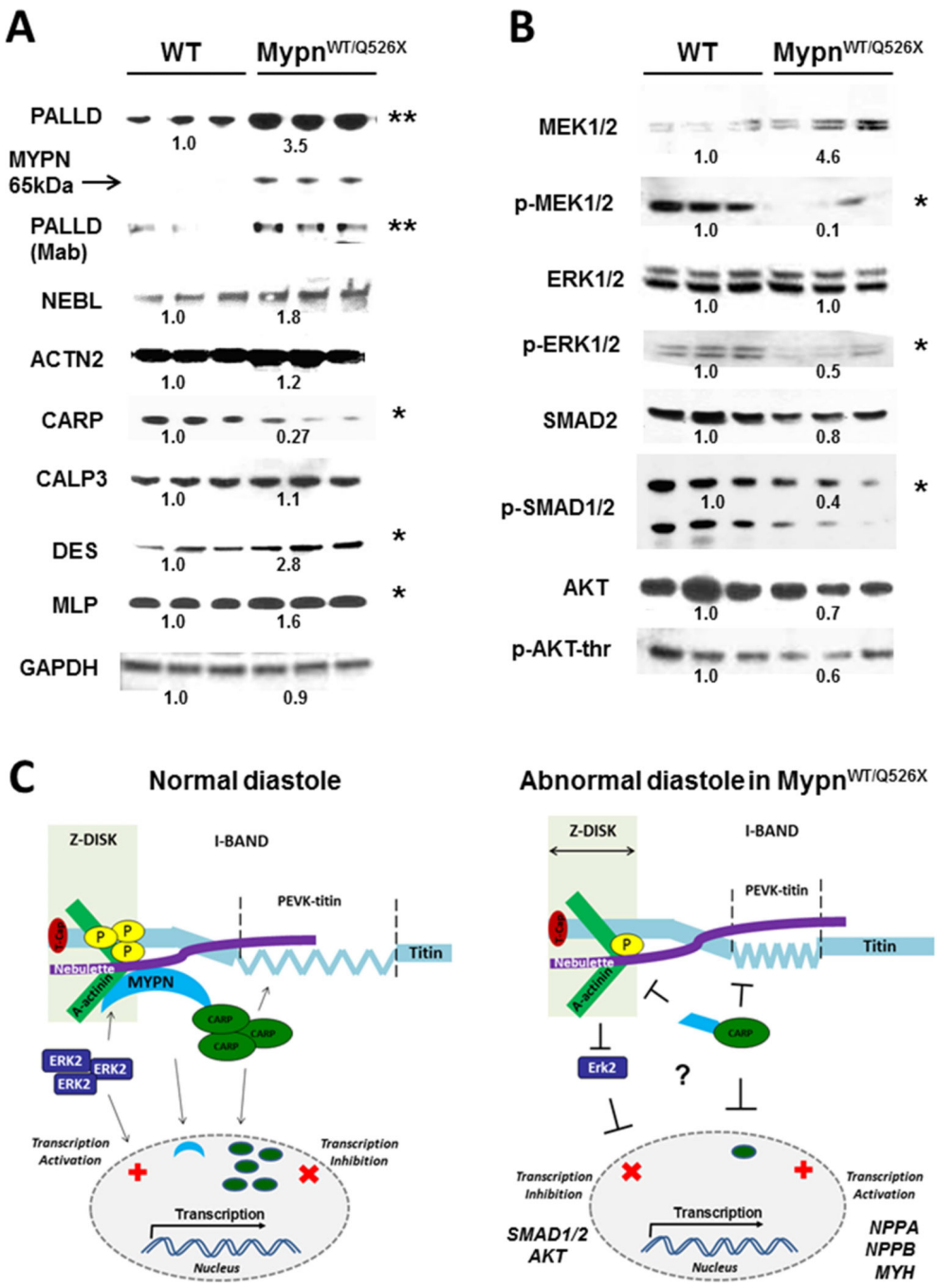

FIGURE 4. Protein Analysis of Mouse Hearts

(A-B) Western blotting images of WT (left lanes) and Mypn$^{WT/Q526X}$ (right lanes) hearts. Significant changes in protein expression from WT were indicated in fold changes in relative density. Expression of 65kDa-Mypn^{Q526X} peptide is indicated by the arrow. Glyceraldehyde 3-phosphate dehydrogenase (GAPDH) was used as a reference protein. **(C)** Hypothetical pathogenic mechanisms of diastolic dysfunction caused by the heterozygous Mypn-Q526X mutation. The **left panel** depicts an idealized model of normal diastolic function. MYPN-CARP at “the central I-band” mechano-transmits the titin-PEVK-based

myofibrillar stress/strain signals to the nucleus. MYPN connects with nebulette-SH3 and α-actinin (ACTN2), further interacting with actin, γ-filamin and titin-Z-repeats, which are dependent on ERK2 phosphorylation. In $Mypn^{WT/Q526X}$ mouse **(right panel)**, levels of mechanosensory molecules are perturbed. CARP and MEK1/2-ERK1/2 are reduced; MLP and DES are up-regulated. CARP-dependent genes such as *NPPA*, *NPPB*, and *MYH* are up-regulated, while ERK1/2-downstream genes, *SMAD1/2* and *AKT*, are down-regulated.
*****$p < 0.05$; ******$p < 0.01$.
CALP3 = calpain3; ERK = extracellular-signal-regulated kinase; MEK = mitogen-activated protein kinase; MLP = muscle LIM protein; NEBL = nebulette; PALLD = palladin; other abbreviations as in **Figures 1 and 3**.

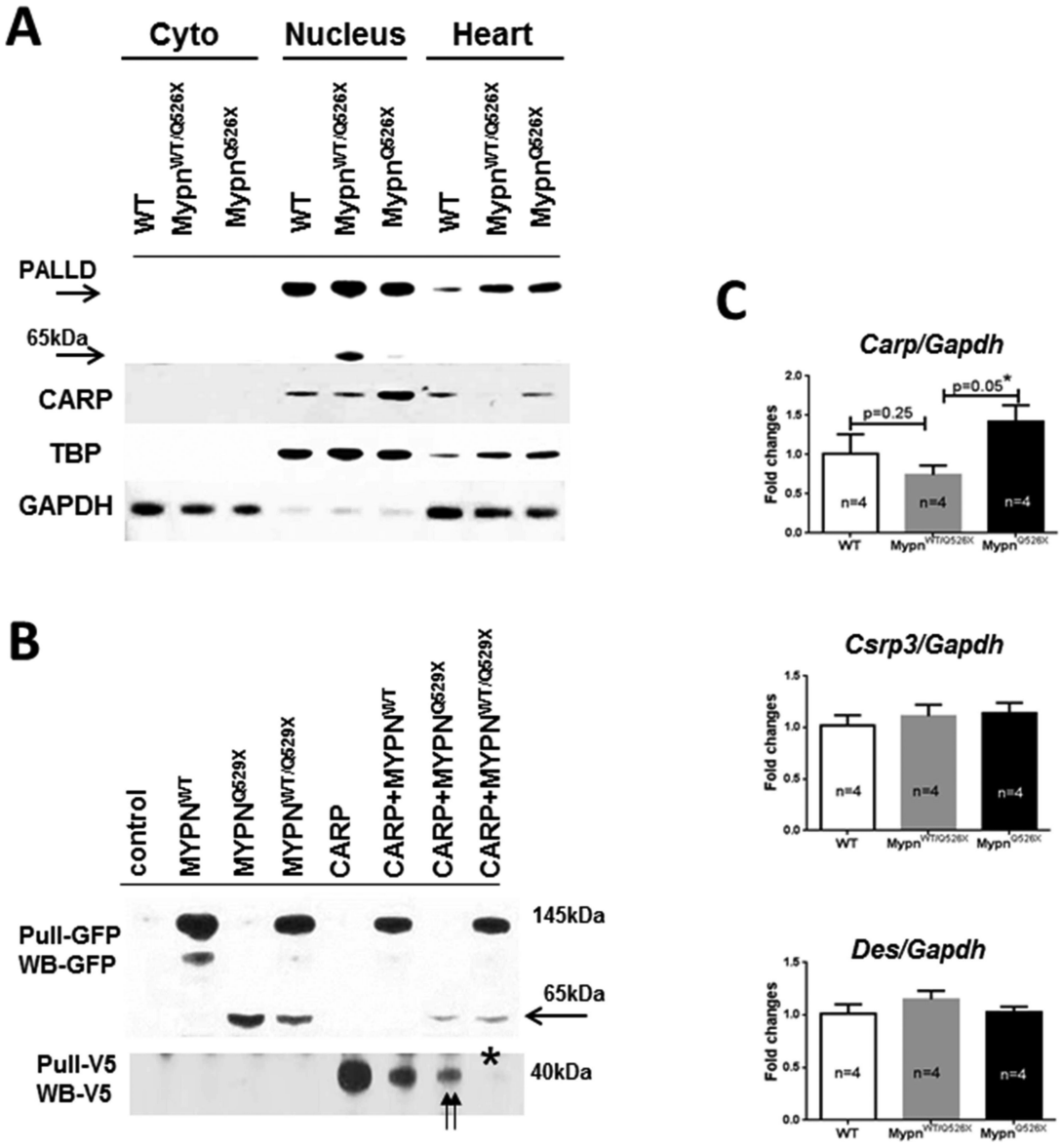

FIGURE 5. Expression and Interaction of MYPN and CARP

(A) Levels of MYPN and CARP in cytoplasmic and nuclear fractions and whole lysates of mouse hearts. GAPDH was used as a cytosolic reference, and TATA-box binding protein (TBP) as a nuclear reference protein. The 65kDa-Mypn^{Q526X} peptide was detected (arrow) in the nucleus and total CARP decreased in Mypn$^{WT/Q526X}$ hearts. The 65kDa-Mypn^{Q526X} peptide is degraded, while levels of nuclear CARP are increased in Mypn^{Q526X} samples. **(B)** Immunoprecipitation studies in HEK293 cells. The expressed human proteins were pulled down with anti-GFP or anti-V5 antibodies and detected by Western blotting with anti-GFP (upper panel) or with anti-V5 (lower panels). Reduced levels of pulled-down 65kDa-MYPN^{Q529X} compared to 145kDa-MYPN^{WT} protein in MYPN^{Q529X} cells and MYPN$^{WT/Q529X}$ mixtures are indicated by arrow. Double arrows indicate reduced levels of 40kDa-CARP-V5 in MYPN^{Q529X} cells compared to MYPN^{WT} cells suggestive for suppressive effects of mutant MYPN^{Q529X} on CARP levels. Asterisks indicate a failure of

anti-V5 in pulling the 40kDa-CARP-V5 in the MYPN$^{WT/Q529X}$ mixture. **(C)** Levels of mRNA of *Carp*, *Mlp/Csrp3*, and *Des* in mouse hearts expressed in fold changes relative to levels of *Gapdh* in WT mice. Results are obtained in a triple from n = 4 mice/group. Csrp = cysteine and glycine-rich protein 3; HEK = human embryonic kidney; mRNA = messenger ribonucleic acid; other abbreviations as in **Figures 1, 3, and 4**.